Timing and Climatic Consequences of the Opening of Drake Passage

Howie D. Scher* and Ellen E. Martin

Age estimates for the opening of Drake Passage range from 49 to 17 million years ago (Ma), complicating interpretations of the relationship between ocean circulation and global cooling. Secular variations of neodymium isotope ratios at Agulhas Ridge (Southern Ocean, Atlantic sector) suggest an influx of shallow Pacific seawater approximately 41 Ma. The timing of this connection and the subsequent deepening of the passage coincide with increased biological productivity and abrupt climate reversals. Circulation/productivity linkages are proposed as a mechanism for declining atmospheric carbon dioxide. These results also indicate that Drake Passage opened before the Tasmanian Gateway, implying the late Eocene establishment of a complete circum-Antarctic pathway.

Over the past 50 million years (My), deterioration of the early Cenozoic greenhouse climate occurred in a series of steps, the largest being widespread and permanent glaciation of Antarctica ~34 Ma (*1*). Changes in ocean circulation and decreasing carbon dioxide (CO_2) levels may have both contributed to the "greenhouse-icehouse" climate transition; however, their relative roles in planetary cooling are currently a matter of debate (*2*). The separation of South America from Antarctica and subsequent formation of Drake Passage are widely believed to have influenced Cenozoic cooling because these events enabled the development of the Antarctic Circumpolar Current (ACC) (*3*). This wind-driven current facilitates interocean exchange of seawater, contributes to upwelling-induced productivity in the Southern Ocean, and is speculated to have reduced poleward heat transport to Antarctica (*4*). However, age estimates for the development of this Pacific-Atlantic connection range from the middle Eocene (*5*) to early Miocene (*3*), obscuring the ACC's role in Antarctic glaciation. Uncertainty over the history of Drake Passage's origin represents a major gap in our knowledge of the primary mechanisms leading to Cenozoic global cooling.

Previous studies have interpreted widespread increases in the biological productivity of the Southern Ocean in terms of the efficiency of circulation-driven nutrient upwelling during the Eocene (*6*, *7*). However, attempts to infer the onset of the ACC from proxies for productivity in the Atlantic sector's sedimentary record are criticized for being equivocal with respect to the opening of Drake Passage (*8*). Ideally, characteristic signatures of Pacific seawater entering the Atlantic sector of the Southern Ocean would provide a sound basis for establishing an age for the Pacific-Atlantic connection.

Neodymium (Nd) isotopes can be used to track changes in ocean circulation because seawater Nd has a short residence time [500 to 1000 years (*9*)] relative to ocean mixing time scales (~1500 years). Water masses are imprinted with the signature of Nd isotope ratios ($^{143}Nd/^{144}Nd$, expressed as ε_{Nd} values) from their source regions, and seawater ε_{Nd} values (*10*) can be used to detect Pacific seawater in the Atlantic sector. Seawater ε_{Nd} values reflect the age of continental Nd inputs to the ocean. The geologic distribution of young volcanic rocks in the circum-Pacific and much older terrains around the Atlantic results in distinct ε_{Nd} values for each basin. Specifically, Pacific ε_{Nd} values are more radiogenic (i.e., positive) than Atlantic values, creating a steep Pacific-Atlantic gradient (*11*).

Ferromanganese (Fe-Mn) crusts and fossil fish teeth preserve ε_{Nd} values of bottom water on tectonic time scales. Early Cenozoic ε_{Nd} values reported for the Pacific Ocean range from –3 to –5 (*12*), whereas values for deep water in the Atlantic sector were less radiogenic [$\varepsilon_{Nd} = -9$ (*13*)]. These records indicate that a steep Pacific-Atlantic ε_{Nd} gradient also existed during the Eocene; thus, an influx of Pacific seawater after the opening of Drake Passage should be clearly resolvable in Atlantic sector ε_{Nd} records. In this study, Nd isotopes in fossil fish teeth from a sediment core on Agulhas Ridge [Ocean Drilling Program (ODP) Site 1090; 3700 m Eocene paleodepth (Fig. 1)] (*14*) are used to evaluate middle Eocene to early Oligocene Atlantic sector ε_{Nd} values (*10*). Fossil fish teeth preserve the same benthic Nd signal as Fe-Mn crusts, but at higher resolution and with better chronologic control (*15*) (table S1).

Nd isotope data from middle to late Eocene fossil fish teeth from Site 1090 (table S2) reveal a transition from nonradiogenic to radiogenic ε_{Nd} values (Fig. 2). From 43 to 41.3 Ma, ε_{Nd} values average –8.2. Between 41.3 and 39.6 Ma, values increase by 2.2 ε_{Nd} units. Late middle Eocene ε_{Nd} values average –6.4. After the transition to more Pacific-like compositions, ε_{Nd} values do not decrease below –6.7 for the remainder of the Eocene, with the most radiogenic ε_{Nd} values occurring during the late Eocene (averaging –6.0).

This paper focuses on the prominent middle Eocene transition to radiogenic ε_{Nd} values. It is the largest ε_{Nd} shift documented in an early Cenozoic Nd isotope record. Low yields of fossil fish teeth during the late middle Eocene limit dating of the onset of the shift to 41.3 to 39.6 Ma. A smaller increase in ε_{Nd} values has also been documented on Maud Rise (ODP Site 689; 1600 m Eocene paleodepth) over this same time interval (*16*) (Fig. 2). Radiogenic ε_{Nd} values do not evolve identically at these locations because of vertical and horizontal offsets; within the limitation of age constraints (*10*), the onset of radiogenic values occurred up to 1.7 My earlier at the shallower site. Regardless, the nearly coeval onset of radiogenic ε_{Nd} values suggests that the shift reflects a regional event.

To place Atlantic sector ε_{Nd} variability in a global paleoceanographic framework, average ε_{Nd} values were calculated from published Nd isotope records for all major ocean basins during three time slices corresponding to the early middle, late middle, and late Eocene (table S3). Resulting values were mapped onto tectonic reconstructions (Fig. 1). Although average ε_{Nd} values at ODP Site 1090 increase from –8.2 to –6, ε_{Nd} values in other ocean basins fluctuate by less than 1 ε_{Nd} unit, and average values in the Pacific and Atlantic Oceans decrease slightly. Thus, the onset of radiogenic ε_{Nd} values in the Atlantic sector of the Southern Ocean was clearly not driven by changes originating in other ocean basins. Rather, the Nd isotopic results provide evidence for the direct introduction of radiogenic Nd into the Atlantic sector during the late middle Eocene.

Seawater ε_{Nd} values can be altered by a change in weathering inputs to the ocean or by water mass mixing. A change in weathering inputs is not likely to account for the required addition of radiogenic material, because major sources of riverine and eolian material to the Atlantic sector are predominantly nonradiogenic (*17*). The only exception is volcanogenic ash derived from sources in the Scotia Sea; such ash is highly reactive and has extremely radiogenic ε_{Nd} values. Ash dispersal into Southern Ocean deep water formation areas (such as the Atlantic sector) may have raised the ε_{Nd} value of deep waters, ultimately carrying the radiogenic signal to Agulhas Ridge. Two observations argue against this mechanism as an explanation for our results. First, there is no evidence of ash deposition in middle Eocene sections of Atlantic sector sediment cores. Second, the ε_{Nd} value of Antarctic Bottom Water (AABW), as recorded by a Fe-Mn crust in Cape Basin (6854-6; Fig. 1) (*18*), changed very little during the late Neogene, despite extensive ash deposition in the Weddell Sea from Scotia Sea volcanism (*19*).

The preferred explanation for the middle Eocene onset of Atlantic sector radiogenic ε_{Nd} values is a change in ocean circulation that brought radiogenic Pacific seawater into the Atlantic sector. Nonradiogenic ε_{Nd} values in the Atlantic sector during the early middle Eocene ($\varepsilon_{Nd} = -8.2$) are consistent with $\delta^{13}C$ and ε_{Nd} reconstructions of deep water circulation that indicate a predominant, Southern Ocean–sourced, deep water mass in the Atlantic (*13*, *20*). Pacific seawater is the only water mass that could have mixed with deep water

Department of Geological Sciences, University of Florida, Gainesville, FL 32611, USA.

*To whom correspondence should be addressed at the Department of Earth and Environmental Sciences, University of Rochester, Rochester, NY 14627, USA. E-mail: howie@earth.rochester.edu

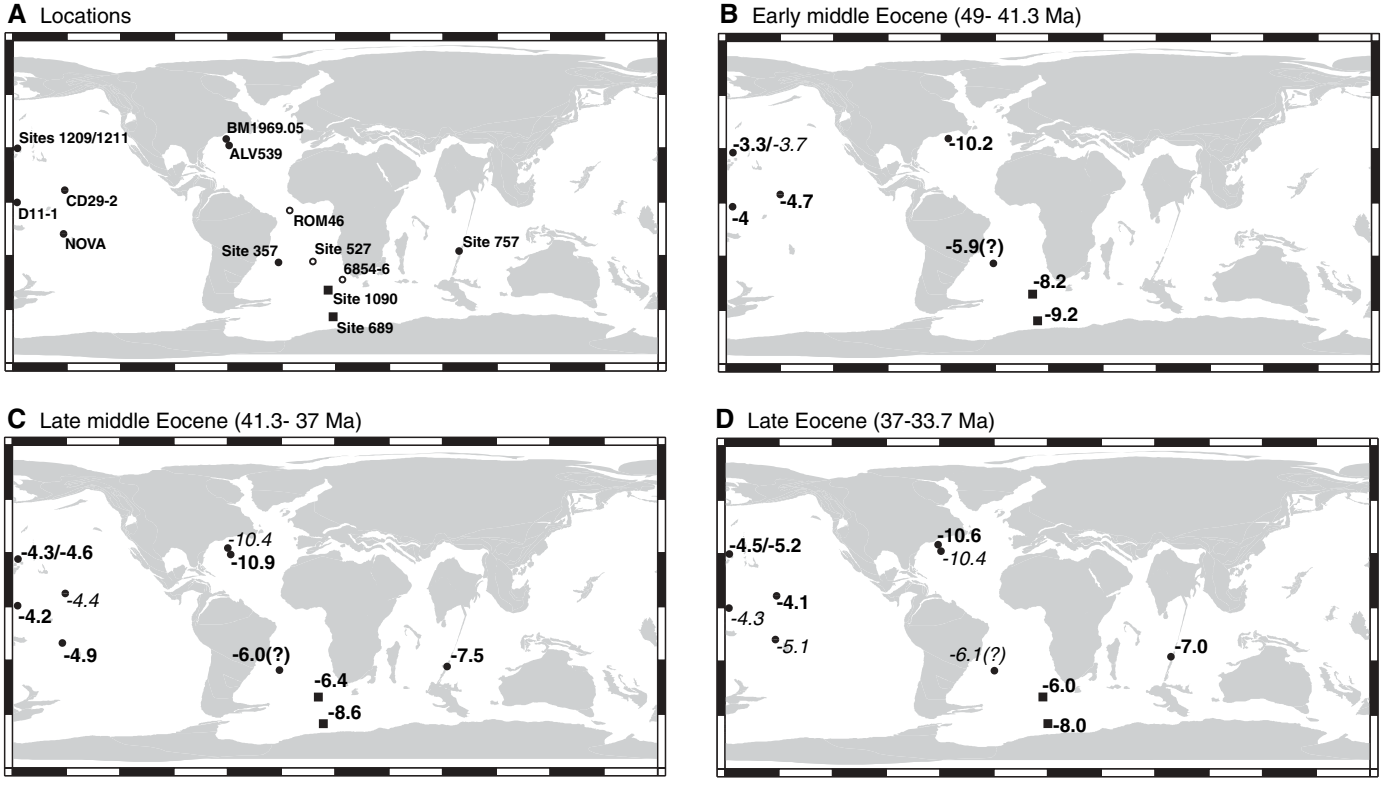

Fig. 1. Plate tectonic reconstructions illustrating locations of ε_{Nd} records and the time-progressive evolution of worldwide seawater ε_{Nd} values from the early middle Eocene, late middle Eocene, and late Eocene. Atlantic sector ODP Sites 1090 and 689 are designated by solid squares. (**A**) Locations of ODP Site 1090 and other relevant sediment cores and Fe-Mn crusts on a late Eocene plate tectonic reconstruction. Solid circles distinguish locations with middle to late Eocene Nd isotope records. Open circles correspond to locations of older and younger Nd isotope records that are discussed in the text. (**B** to **D**) Numbers represent the arithmetic mean of Nd isotope data from samples falling within the corresponding time interval. Numbers in italics represent a linear interpolation through the midpoint of the time interval using adjacent data points (table S3). Sources of the Nd isotope data used in this figure are contained in table S3.

sourced in the Southern Ocean to generate ε_{Nd} values as high as –6.0 on Agulhas Ridge.

Based on Eocene paleogeography, Pacific seawater could have entered the Atlantic sector through the Indian Ocean or via the Central American Seaway (CAS); however, there are arguments against these pathways. Benthic foraminiferal $\delta^{13}C$ records from the Indian Ocean indicate that the Ninetyeast Ridge was an effective barrier to deep water communication between the western and eastern Indian Ocean for depths below 2000 m (*21*). Furthermore, ε_{Nd} values from a shallow location on Ninetyeast Ridge (ODP Site 757; Fig. 1) do not suggest the influence of Pacific water (*22*). Similarly, South Atlantic ε_{Nd} records from the Romanche Fracture Zone (ROM46; Fig. 1) (*23*) and Walvis Ridge [Deep Sea Drilling Program (DSDP) Site 527; Fig. 1] (*13*) do not suggest a Pacific influence during the early Cenozoic. The Rio Grande Rise (DSDP Site 357; Fig. 1) exhibits radiogenic ε_{Nd} values during the Eocene (Fig. 1) (*24*); however, these values are called into question because there is a volcanic breccia layer in middle Eocene sediments that may have contributed radiogenic Nd to Fe-Mn coatings on uncleaned foraminifera.

It is likely that the abrupt appearance of Pacific-like ε_{Nd} values in Atlantic sector records reflects the early opening of Drake Passage ~41 Ma. This conclusion corroborates recent findings of an eightfold increase in spreading rate that accompanied a change in spreading direction between South America and Antarctica ~50 Ma (*5*). Positive shifts in ε_{Nd} records from the Atlantic sector, ~9 My after the new phase of spreading, indicate that crustal extension and thinning led to the development of a Pacific-Atlantic connection that could be exploited by wind-driven Pacific seawater throughflow. We believe that the strong radiogenic signal observed at Agulhas Ridge reflects the influx of radiogenic Nd through Drake Passage into deep water production areas of the Southern Ocean. The observation that ODP Site 689 shows a weaker response to the early opening of Drake Passage, despite being located closer to Pacific throughflow and having a shallower Eocene paleodepth, implies that water masses were vertically stratified in the Atlantic sector, with Southern Ocean deep water lying below intermediate depths on Maud Rise. Pronounced vertical gradients in water mass properties have been previously documented between intermediate and deep locations in the Atlantic sector during the middle to late Eocene (*25*).

Today 60% of AABW forms in the Atlantic sector, mostly in the Weddell Sea. From there, the bottom water is exported to the north via the Scotia Sea, though some is recirculated within the Weddell gyre and carried toward Maud Rise (*26*). It is possible that Pacific seawater entered the Atlantic sector, sank during deep water production in the Weddell Sea, and was transported to Agulhas Ridge. However, this seawater may have had less of an effect at Maud Rise because (i) the Weddell gyre was absent or not well organized in the Eocene, or (ii) the relatively shallow paleodepth of ODP Site 689 meant that it was influenced by water masses forming elsewhere; i.e., in areas less affected by Pacific seawater. It is also possible that the development of fronts, which are water mass boundaries for surface water, influenced the distribution of ε_{Nd} values in Atlantic sector surface waters. Reconstructions of Eocene paleofront positions based on microfossil distributions indicate a proto-Polar Front very close to Maud Rise (*27*), a front whose existence is supported by large variations in paleoproductivity during the middle Eocene (*6*).

Changes in Atlantic sector ε_{Nd} values outline the history of the opening of Drake Passage more directly than previous studies that relied on other paleoceanographic proxies to infer a Pacific-Atlantic connection. The early opening ~41 Ma is documented by the onset of radiogenic values in the Atlantic sector. Under the assumption that a greater volume of Pacific throughflow resulted in more radiogenic Atlantic sector ε_{Nd} values, subsequent ε_{Nd} increases during the late Eocene most

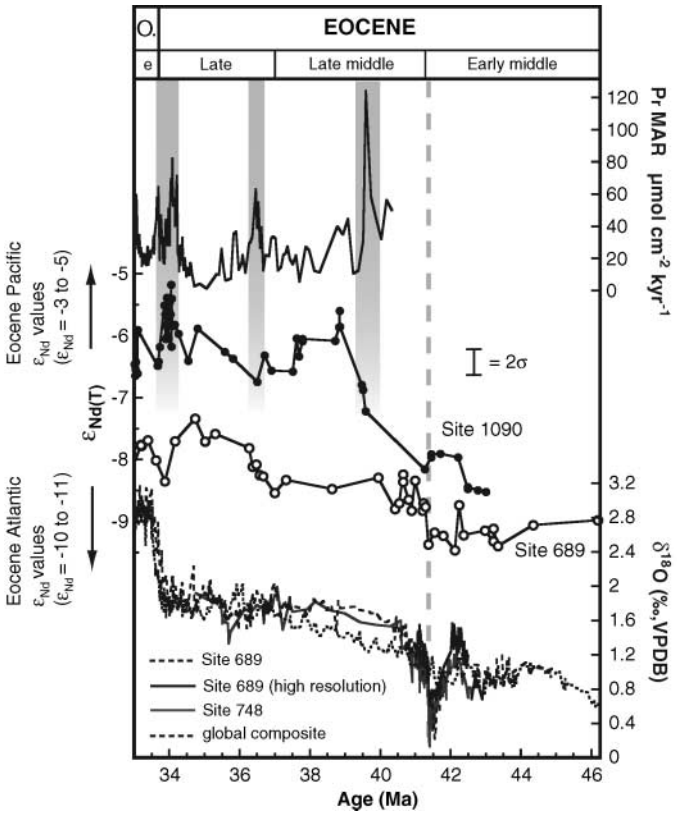

Fig. 2. Nd isotope records, temperature and ice volume, and productivity proxy records from Atlantic and Indian sector sediment cores, and the global composite $\delta^{18}O$ record for the middle Eocene to early Oligocene. (**Top**) Reactive phosphorus mass accumulation rate (P_r MAR) data for ODP Site 1090 from Anderson and Delaney (*14*), including early middle Eocene data from their auxiliary material that has been plotted according to the extended chronology for ODP Site 1090 described in table S1. (**Middle**) ε_{Nd} records for Sites 1090 (solid circles) and 689 (open circles). The error bar represents 2σ external reproducibility (*10*). The Eocene range of Pacific and Atlantic ε_{Nd} values are noted on the left *y* axis. (**Bottom**) $\delta^{18}O$ values for the global composite and ODP Sites 689 (Maud Rise) and 748 (Kerguelen Plateau). All Southern Ocean $\delta^{18}O$ data are from *Cibicidoides* spp. reported relative to the Vienna Pee Dee belemnite standard (‰ VPDB) and have been adjusted by + 0.64 ‰ to account for vital effects. Sources of $\delta^{18}O$ data are as follows: ODP Site 689 (*6*); ODP Site 689, high resolution; and ODP Site 748 (*31*), global composite (*1*). Gray bars highlight inferred associations between changes in ocean circulation and sea surface productivity in the Atlantic sector. The vertical dashed gray line highlights the onset of radiogenic ε_{Nd} values and the termination of the MECO (*31*).

likely represent progressive widening and deepening of the gateway. A pronounced ε_{Nd} increase at Maud Rise ~37 Ma has been previously interpreted as an opening of Drake Passage to intermediate depths (*16*). An increase in Pacific throughflow ~34 Ma is indicated by a shift to the most radiogenic values observed at Agulhas Ridge and is interpreted as the establishment of a deeper Pacific-Atlantic connection in the late Eocene. This conclusion is supported by tectonic reconstructions (*28*). Alternatively, increased deepening of the Tasmanian Gateway from 35.5 to 33.5 Ma (*29*) may have initiated greater throughflow via Drake Passage without a substantial change in its dimensions. Lower ε_{Nd} values during the earliest Oligocene are part of a long-term decrease in ε_{Nd} in response to global circulation changes. This trend was also observed at ODP Site 689 (*16*).

Chemical proxies for export productivity (*7*) and organic carbon burial (*14*) in middle to late Eocene Atlantic sector sediments demonstrate a long-period cycle. High values, centered around 39, 36.5, and 34.6 to 33.6 Ma (*14*, *30*), coincide with increasing ε_{Nd} values (Fig. 2). We speculate that changes in circulation, initiated by the early opening and successive deepening of Drake Passage, enhanced nutrient upwelling. These changes appear to have stimulated the biological pump, which is an important link between short- and long-term carbon cycles. This mechanism may have been a factor in lowering atmospheric CO_2 during the Paleogene. The influence of this mechanism on global climate may be evident during the middle Eocene, when an ephemeral glaciation, associated with changes in carbon cycling (*31*), followed an enigmatic climate reversal called the middle Eocene climatic optimum (MECO) (*32*). Cooling coincided with the early opening of Drake Passage (Fig. 2).

Nd isotope results suggest that Drake Passage opened before the Tasmanian Gateway. Reduction of oceanic heat flux after ACC development (*4*) is not unanimously accepted as a mechanism for global cooling (*29*); however, our results imply that a circum-Antarctic pathway could have existed by the late Eocene. Additionally, the proposed circulation-induced productivity increase may have sequestered atmospheric CO_2, contributing to global cooling and Antarctic glaciation.

References and Notes

1. J. Zachos, M. Pagani, L. Sloan, E. Thomas, K. Billups, *Science* **292**, 686 (2001).
2. R. M. DeConto, D. Pollard, *Nature* **421**, 245 (2003).
3. P. F. Barker, *Earth Sci. Rev.* **55**, 1 (2001).
4. J. P. Kennett, *J. Geophys. Res.* **82**, 3843 (1977).
5. R. Livermore, A. Nankivell, G. Eagles, P. Morris, *Earth Planet. Sci. Lett.* **236**, 459 (2005).
6. L. Diester-Haass, R. Zahn, *Geology* **24**, 163 (1996).
7. J. C. Latimer, G. M. Filippelli, *Palaeogeogr. Palaeoclimatol. Palaeoecol.* **182**, 151 (2002).
8. P. Barker, E. Thomas, *Earth Sci. Rev.* **66**, 143 (2004).
9. K. Tachikawa, V. Athias, C. Jeandel, *J. Geophys. Res.* **108**, 3254 (2003).
10. Materials and methods are available as supporting material on *Science* Online.
11. S. L. Goldstein, S. R. Hemming, in *The Oceans and Marine Geochemistry*, H. Elderfield, Ed. (Elsevier, Oxford, 2003), pp. 453–489.
12. H. F. Ling *et al.*, *Earth Planet. Sci. Lett.* **146**, 1 (1997).
13. D. J. Thomas, T. J. Bralower, C. E. Jones, *Earth Planet. Sci. Lett.* **209**, 309 (2003).
14. L. D. Anderson, M. L. Delaney, *Paleoceanography* **20**, PA1013 (2005).
15. E. E. Martin, H. D. Scher, *Earth Planet. Sci. Lett.* **220**, 25 (2004).
16. H. D. Scher, E. E. Martin, *Earth Planet. Sci. Lett.* **228**, 391 (2004).
17. S. L. Goldstein, R. K. O'Nions, P. J. Hamilton, *Earth Planet. Sci. Lett.* **70**, 221 (1984).
18. M. Frank, N. Whiteley, S. Kasten, J. R. Hein, K. O'Nions, *Paleoceanography* **17**, 10.1029/2000PA000606 (2002).
19. H. W. Hubberten, W. Morche, F. Westall, D. K. Fuetterer, J. Keller, *Proc. Ocean Drilling Program Sci. Res.* **114**, 733 (1991).
20. K. G. Miller, in *Eocene-Oligocene Climatic and Biotic Evolution*, D. Prothero, W. A. Berggren, Eds. (Princeton Univ. Press, Princeton, NJ, 1992), pp. 160–177.
21. J. C. Zachos, D. K. Rea, K. Seto, R. Nomura, N. Niitsuma, in *The Indian Ocean: A Synthesis of Results from the Ocean Drilling Program*, R. A. Duncan, D. K. Rea, R. B. Kidd, U. von Rad, J. K. Weissel, Eds. (American Geophysical Union, Washington, DC, 1992), pp. 351–386.
22. H. D. Scher, E. E. Martin, A. A. Haase, *Geochim. Cosmochim. Acta* **66**, A677 (2002).
23. M. Frank *et al.*, *Paleoceanography* **18**, PA1091 (2003).
24. M. R. Palmer, H. Elderfield, *Geochim. Cosmochim. Acta* **50**, 409 (1986).
25. G. A. Mead, D. A. Hodell, P. F. Cielcielski, in *The Antarctic Paleoenvironment: A Perspective on Global Change*, J. P. Kennett, D. A. Warnke, Eds. (American Geophysical Union, Washington, DC, 1993), pp. 27–48.
26. A. H. Orsi, G. C. Johnson, J. L. Bullister, *Prog. Oceanogr.* **43**, 55 (1999).
27. P. J. Cooke, C. S. Nelson, M. P. Crundwell, D. Spiegler, *Palaeogeogr. Palaeoclimatol. Palaeoecol.* **188**, 73 (2002).
28. L. A. Lawver, L. M. Gahagan, *Palaeogeogr. Palaeoclimatol. Palaeoecol.* **198**, 11 (2003).
29. C. E. Stickley *et al.*, *Paleoceanography* **19**, PA4027 (2004).
30. The peak in reactive phosphorus mass accumulation rate (P_r MAR) at 39 Ma may be an artifact of a change in sedimentation rate that is not resolved in the extended age model (*10*) but is possibly indicated by other proxy records (*33*). However, the occurrence of the peak at 39 Ma appears to be part of a cycle of high- and low-productivity intervals observed at this location (*14*).
31. A. Tripati, J. Backman, H. Elderfield, P. Ferretti, *Nature* **436**, 341 (2005).
32. S. M. Bohaty, J. C. Zachos, *Geology* **31**, 1017 (2003).
33. L. Anderson, personal communication.

34. This manuscript benefited from discussions with P. Barker, S. Blair, S. Bohaty, D. Hodell, A. Piotrowski, and J. Smellie; laboratory assistance from A. Heatherington and R. Thomas; and thoughtful reviews by three anonymous referees. This study was supported by NSF grant OCE-962970 to E.E.M. Samples used in this study were provided by the ODP.

Supporting Online Material

www.sciencemag.org/cgi/content/full/312/5772/428/DC1
Materials and Methods
Tables S1 to S3

12 September 2005; accepted 21 March 2006
10.1126/science.1120044

Timing and Climatic Consequences of the Opening of Drake Passage

Howie D. Scher and Ellen E. Martin

Science **312**, 428 (2006);
DOI: 10.1126/science.1120044